

Aberystwyth University

Paleo-ENSO influence on African environments and early modern humans

Kaboth-Bahr, Stefanie; Gosling, William D.; Vogelsang, Ralf; Bahr, André; Scerri, Eleanor M.L.; Asrat, Asfawossen; Cohen, Andrew S.; Düsing, Walter; Foerster, Verena; Lamb, Henry F.; Maslin, Mark A.; Roberts, Helen M.; Schäbitz, Frank; Trauth, Martin H.

Published in:

Proceedings of the National Academy of Sciences of the United States of America

DOI:

[10.1073/pnas.2018277118](https://doi.org/10.1073/pnas.2018277118)

Publication date:

2021

Citation for published version (APA):

Kaboth-Bahr, S., Gosling, W. D., Vogelsang, R., Bahr, A., Scerri, E. M. L., Asrat, A., Cohen, A. S., Düsing, W., Foerster, V., Lamb, H. F., Maslin, M. A., Roberts, H. M., Schäbitz, F., & Trauth, M. H. (2021). Paleo-ENSO influence on African environments and early modern humans. *Proceedings of the National Academy of Sciences of the United States of America*, 118(23), [e2018277118]. <https://doi.org/10.1073/pnas.2018277118>

Document License

CC BY-NC

General rights

Copyright and moral rights for the publications made accessible in the Aberystwyth Research Portal (the Institutional Repository) are retained by the authors and/or other copyright owners and it is a condition of accessing publications that users recognise and abide by the legal requirements associated with these rights.

- Users may download and print one copy of any publication from the Aberystwyth Research Portal for the purpose of private study or research.
- You may not further distribute the material or use it for any profit-making activity or commercial gain
- You may freely distribute the URL identifying the publication in the Aberystwyth Research Portal

Take down policy

If you believe that this document breaches copyright please contact us providing details, and we will remove access to the work immediately and investigate your claim.

tel: +44 1970 62 2400
email: is@aber.ac.uk



Supplementary Information for

Paleo-ENSO influence on African environments and early modern humans

Stefanie Kaboth-Bahr^{1,2*}, William D. Gosling³, Ralf Vogelsang⁴, André Bahr², Eleanor Scerri^{5,6}, Asfawossen Asrat⁷, Andrew S. Cohen⁸, Walter Düsing¹, Verena E. Foerster⁹, Henry F. Lamb^{10,11}, Mark A. Maslin^{12,13}, Helen M. Roberts¹⁰, Frank Schäbitz⁹, Martin H. Trauth¹

¹ University of Potsdam, Institute of Geosciences, Potsdam, Germany

² University Heidelberg, Institute of Earth Sciences, Heidelberg, Germany

³ University of Amsterdam, Institute for Biodiversity and Ecosystem Dynamics, Amsterdam, Netherlands

⁴ University of Cologne, Department of Prehistoric Archaeology, Cologne, Germany

⁵ Pan-African Evolution Research Group, Max Planck Institute for the Science in Human History, Jena, Germany

⁶ Department of Classics and Archaeology, University of Malta, Msida, Malta

⁷ Addis Ababa University, School of Earth Sciences, Addis Ababa, Ethiopia

⁸ University of Arizona, Department of Geosciences, Tucson, USA

⁹ University of Cologne, Institute of Geography Education, Cologne, Germany

¹⁰ Aberystwyth University, Department of Geography and Earth Sciences, Aberystwyth, UK

¹¹ University of Dublin, Trinity College, Department of Botany, Dublin, Ireland

¹² University College London, Department of Geography, London, UK

¹³ Natural History Museum of Denmark, University of Copenhagen, Copenhagen, Denmark

Email: Stefanie Kaboth-Bahr; kabothbahr@uni-potsdam.de

This PDF file includes:

Supplementary text
Figures S1 to S3
Tables S1 to S4
SI References

Supplementary Information Text

Site and proxy selection

For the pan-African proxy moisture reconstruction during the Middle and Upper Pleistocene, we selected nine established marine and terrestrial sedimentary archives that meet a number of critical prerequisites: (i) the sites need to be sensitive to moisture changes on the African continent, (ii) sufficient age control must be provided, (iii) the proxy record must at least cover half of the investigated time period of the last ~620 kyr, and (iv) the temporal data resolution should be <5 kyrs to provide sufficient data points for further statistical analysis. We retained the published age model of each individual record as well as their initial proxy record interpretation. The proxy records on their individual age models are shown in Figure S1 as well as site details and proxy explanation are provided in Table S1.

Effect of El Niño/La Niña induced Walker Circulation changes on African precipitation

During El Niño (positive ENSO phase), warming of the eastern and central equatorial Pacific causes ascending motion over the central and eastern Pacific and subsidence over Indonesia (see Fig. 1 in the main text) (1). Over the Indian Ocean this atmospheric configuration leads to a weakening or even reversal of the westerlies initiating pooling of warm water in its northwestern part (positive Indian Ocean Dipole phase). As a consequence, eastern Africa experiences increasingly humid conditions due to the adjacent strong convection over the northwestern Indian Ocean. Increased descending mass fluxes on the western side of the African continent at the same time suppress convection and hence cause aridity over its southern parts (see Fig. 1 in the main text) (1). While El Niño is typically initiated during boreal winter over the Indo-Pacific realm, it incites a lagged response during the subsequent spring-summer over the Atlantic Ocean where intensified trade winds cause the development of a cold tongue of upwelling water along the western African shore (see Fig. 1 in the main text; Atlantic Niño) (2). In combination with the dominant subsidence in western Africa, the reduced evaporation over the cooled eastern equatorial Atlantic increases aridity across southern Africa in boreal winter and in addition the Sahel Zone during boreal summer. In phase with the above discussed alterations of the Walker Circulation (WC), the Hadley Circulation (HC) – which transports moisture latitudinally - also weakens in both hemispheres due to reduced moisture ascension in the African tropics (1). The lack of moisture transport through the HC towards the subtropics adds to the drier conditions under El Niño conditions in south and northwestern Africa in the respective hemisphere summer. During La Niña conditions (negative ENSO phase), the entire system reverses from the El Niño scenario (see Fig. 1 in the main text) leading to the development of a negative Indian Ocean Dipole and Atlantic Niña phase (1). In addition to the outlined mechanism the interferences between WC also causes precipitation anomalies during the subsequent summer month which can regionally vary from the winter counterparts. An example is ENSO interference with the Congo Air Boundary which leads during the summer months also to additional rainfall in western Africa from the Sahel to the Congo basin (1). Although ENSO variability most strongly affects the “short rain season during the winter months it nevertheless shifts the yearly precipitation budget of these regions to generally wetter or drier conditions relative to non-El Niño years (3, 4). Hence, the temporal changes in precipitation anomalies during the “long rain” season relative to the “short rain” season does not significantly contribute to the overall annual budget change observed during strong ENSO years.

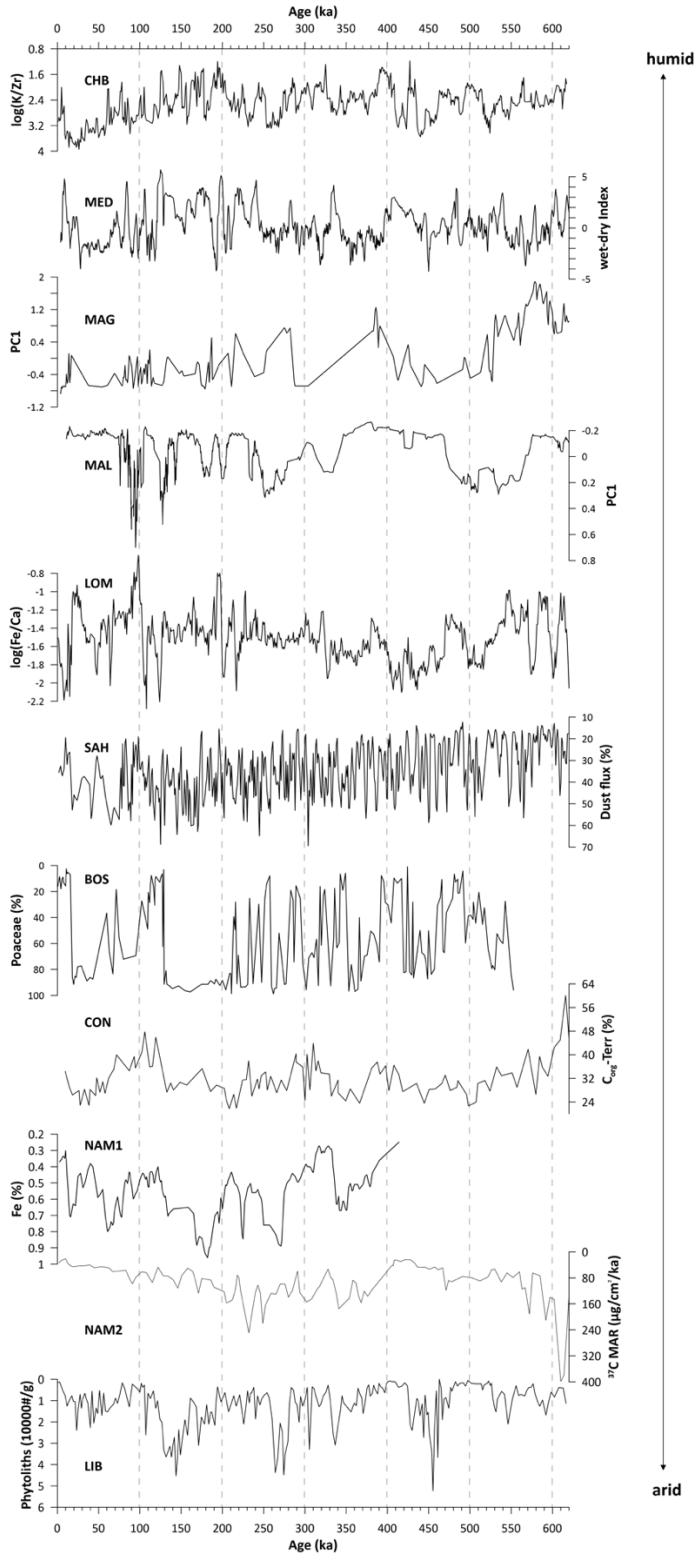


Fig. S1. Overview of the proxy records used for the analysis of pan-African climate change during the last ~620 kyr. All original data sets are presented using their original, published age models. Abbreviations and respective references are listed in Table S1.

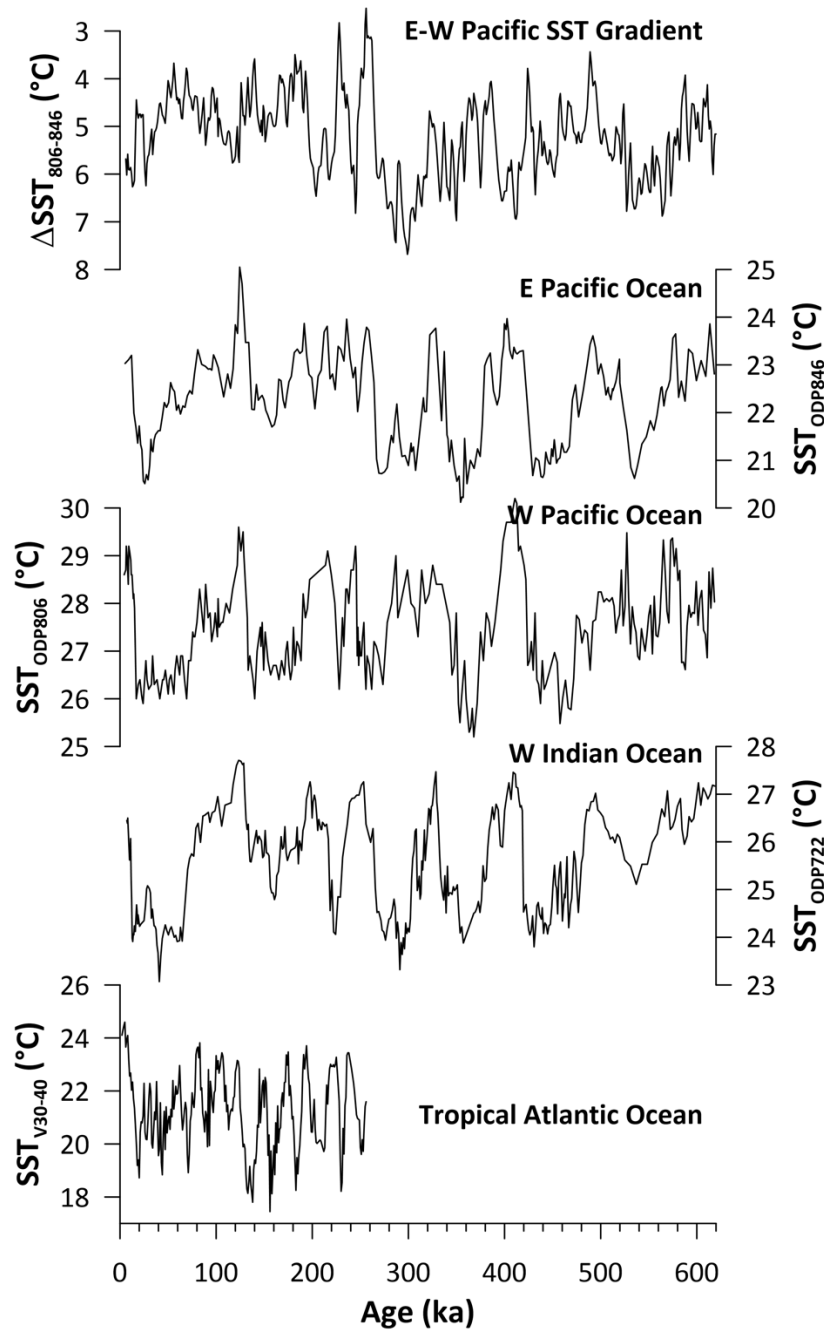


Fig. S2. Overview of the sea-surface temperature (SST) records used for the analysis of El Niño-Southern Oscillation/Walker Circulation changes. All original data sets are presented on their individual age model. Coordinates and respective references are listed in Table S2.

Table S1. Coordinates of African Sites and proxy records used in this study. * denotes marine sediment cores; † denotes terrestrial sediment cores.

Region	Core	Lon (E)	Lat (N)	Age (ka)	Proxy	Proxy interpretation	Reference
MED	ODP967*	29° 39.15'	34° 51.84'	4-620	XRF-based wet-dry index	wet >0 high Nile river run-off; dry <0 low Nile river run-off	(5)
CHB	HSPDP-CHB14-2†	36° 05.00'	4° 01.00'	1-620	log(K/Zr)	wet: high log(K/Zr) values; dry: low log(K/Zr) values	(6)
MAG	HSPDP-MAG14-2A†	36° 16.76'	-01° 51.09'	4-620	Pollen	wet: high PCA1 values of pollen assemblage indicating woodland biome; dry: low PCA1 values of pollen assemblage indicating savannah biome	(7)
MAL	HSDSP-MAL05-1†	34° 24.00'	-11° 12.00'	12-620	PC1	wet: high Lake level; dry low lake level	(8)
LOM	MD96-2048*	34° 01.00'	-26° 10.00'	1-620	log(Fe/Ca)	wet: high terrestrial input via Limpopo river (high Fe/Ca); dry: low terrestrial input via Limpopo river (low Fe/Ca)	(9)
SAH	ODP659*	-21° 01.57'	18° 04.63'	2-620	Dust	Wet: less dust input into the Atlantic Ocean; dry: more dust input into the Atlantic Ocean	(10)
BOS	BOS04-5B†	-1° 02.50'	6° 30.00'	1-552	Poaceae	wet: high Poaceae percentages indicating woodland biome; dry: low Poaceae percentages indicating savannah biome	(11)
CON	ODP1075*	10° 04.98'	-04° 47.11'	9-620	C _{org} -Terr	wet: increased terrigenous organic matter supply by the Congo river to the Congo fan region; dry: decreased terrigenous organic matter supply by the Congo river to the Congo fan region	(12)
NAM 1	GeoB1028-5*	9°11.15'	-20°06.24'	3-413	Fe	wet: low Fe-input through dust plumes into the Atlantic Ocean (Low Fe); dry: high Fe-input through dust plumes into the Atlantic Ocean	(13)
NAM 2	ODP1082*	11° 49.23'	-21° 05.65'	2-620	C ³⁷ MAR	wet: low off-shore productivity (low C ³⁷ MAR) due to low coastal upwelling. The warm SST resulting from the lack of cold-water upwelling lead increased humidity transport into the Namib region; dry: high off-shore productivity (high C ³⁷ MAR) due to high coastal upwelling. The cold SST due to upwelling lead to drought and desertification of Namib region.	(14)
LIB	ODP663*	-11° 52.71'	-1°11.82'	0-620	Phytoliths	Wet: low phytolith concentrations indicate decreased aeolian transport and wetter hinterland conditions; dry: low phytolith concentrations indicate increased aeolian transport and wetter hinterland conditions	(15)

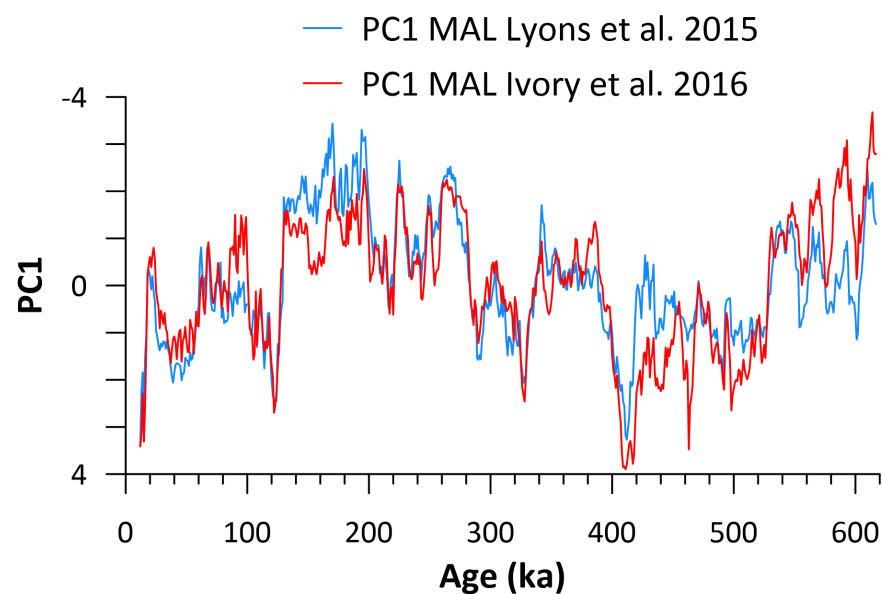


Fig. S3. Comparison of PC1 derived from the piecewise PCA (pwPCA; see methods in main text) of eleven pan-African proxy records using different age models for MAL (see Table S2 for site details). The preferred age model in this study follows (7).

Table S2. Coordinates of sea-surface temperature (SST) records used for the analysis of El Niño-Southern Oscillation/Walker Circulation changes.

Site	Lon (E)	Lat (N)	Reference
ODP 846	-90°49.09'	-3°05.70'	(16)
ODP 806	159°21.66'	0°19.11'	(17)
ODP 722	59°47.71'	16°37.30'	(16)
V30-40	0°12.00'	-23°09.00'	(18)

Table S3. Median calculation of all proxy records used in this study. See Table S1 for site location according to abbreviation. red = arid conditions; blue = humid conditions.

	CHB	MED	MAG	MAL	LOM	SAH	BOS	LIB	CON	NAM1	NAM2
<i>Cut-off</i>	1.09	0.07	-0.04	0.09	-1.49	-1.35	57.75	-1.07	30.29	-0.29	78.96
Phase IV	1.36	-0.91	-0.05	0.15	-1.42	-3.43	20.69	-0.69	30.29	-0.30	46.73
Phase III	1.07	1.12	-0.03	0.03	-1.44	1.72	90.92	-1.81	29.17	-0.21	109.42
Phase II	1.10	-0.10	-0.59	0.09	-1.64	-0.80	49.96	-0.94	32.15	-0.35	78.82

Table S4. Overview of key hominin fossil findings of mid to late Pleistocene age referenced in Figure 3 of the main text.

Location	Age (ka)	References
Bodo D'ar, Ethiopia	600	(19)
Kapthurin Formation, Kenya	509 – 543 (510 - 512)	(20)
Ndutu, Lake Ndutu, Tanzania	490 – 780	(21, 22)
Lainyamok, Kenya	393-300	(23)
Broken Hill, Kabwe 1, Zambia	299 ±25	(24–26)
Cave of Hearth, RSA	200 – 500	(27, 28)
Sidi Abderrahman, La Grottes de Littorine, Morocco	~ 375	(29)
Cameroon	~ 338 (237 – 581)	(30)
Jebel Irhoud, Morocco	315 ± 14	(31, 32)
Dinaledi Chamber, Rising Star Cave System, RSA	236 – 335	(33, 34)
Hoedjiespunt 1, RSA	200 – 300 (125 – 770)	(28, 35)
Florisbad, RSA	224 – 294 (age questioned by Berger & Hawks)	(36–38)
Gawis Cranium, Awash River, Ethiopia	300-500	(39)
Omo Kibish I, II & III, Ethiopia	195 ± 5	(36, 40)
Guomde, East Turkana, Kenya	> 180	(36, 41–43)
Rabat (Kebibat), Morocco	late Middle Pleistocene (125-400)	(36, 44)
Eliye Springs, Kenya	late Middle Pleistocene (125-400)	(36, 45, 46)
El Aliya & Témara, Morocco	Aterian MIS6 (130-190)	(36)
Herto 1 & 2, Ethiopia	154 – 160	(47–50)
Singa, Sudan	131-135	(36, 51–54)
Pinnacle Point 13b, RSA	90 – 100 90 – 162	(55, 56)
Mumba, Tanzania	110 – 130	(57)
Lake Eyasi, Tanzania	88-130	(36, 58, 59)

Grottes de Contrebandiers, Morocco	80-130	(36, 60)
Ysterfontein 1, RSA	71 – 105	(55, 56, 61)
	50 – 130	
Blind River, RSA	112 – 124	(28, 56)
Ngaloba, Laetoli, Tanzania	120 ± 30	(36, 62–65)
Dar-es-Soltan II 5, Morocco	> 110?	(36, 66, 67)
Klasies River Mouth, RSA	100 ± 25	(21, 36, 56)
	85 – 110	
Witkrans, RSA	86 – 103	(28, 56, 68)
	(50 – 100)	
Sea Harvest, RSA	85 – 95	(28, 56, 69)
	(71 – 110)	
Middle Awash, Bouri & Aduma, Ethiopia	79 - 105	(70)
Equus Cave, RSA	30 – 103	(56, 71)
Plovers Lake, RSA	62.9 – 88.7	(55, 56)
	62 – 89	
Die Kelders, Cave 1, RSA	59 – 74	(56, 72)
Taramsa Hill, Egypt	50 – 80	(36, 73, 74)
Border Cave, RSA	61 – 72	(36, 75)
	71 – 91	
	152 – 171?	
Klipdrift Shelter, RSA	60 – 65	(55, 56)
	(52 – 72)	
Haua Fteah, Libya	70	(36, 76)
Blombos Cave, RSA	100 - 94	(28, 56, 77)
	65 – 70	
	70 – 102	
Sibudu, RSA	64 – 77	(55, 56)
Diepkloof Rock Shelter, RSA	58 – 61	(55, 56)
Ndutu, OH 83, Tanzania	32-60	(78)
Hofmeyer, RSA	36	(79)

SI References

1. C. P. de Oliveira, L. Aímola, T. Ambrizzi, A. C. V. Freitas, The Influence of the Regional Hadley and Walker Circulations on Precipitation Patterns over Africa in El Niño, La Niña, and Neutral Years. *Pure Appl. Geophys.* **175**, 2293–2306 (2018).
2. C. Brierley, I. Wainer, Inter-annual variability in the tropical Atlantic from the Last Glacial Maximum into future climate projections simulated by CMIP5/PMIP3. *Clim. Past* **14**, 1377–1390 (2018).
3. I. Fer, B. Tietjen, F. Jeltsch, C. Wolff, The influence of El Niño-Southern Oscillation regimes on eastern African vegetation and its future implications under the RCP8.5 warming scenario. *Biogeosciences* **14**, 4355–4374 (2017).
4. S. M. Moore, *et al.*, El Niño and the shifting geography of cholera in Africa. *Proc. Natl. Acad. Sci. U. S. A.* **114**, 4436–4441 (2017).
5. K. M. Grant *et al.*, A 3 million year index for North African humidity/aridity and the implication of potential pan-African Humid periods. *Quat. Sci. Rev.* **171**, 100–118 (2017).
6. Trauth *et al.*, Recurring types of variability and transitions in the ~620 kyr record of climate change from the Chew Bahir basin, southern Ethiopia. *Quat. Sci. Rev.*, *in press*, doi: 10.1016/j.quascirev.2020.106777
7. R. B. Owen, *et al.*, Progressive aridification in East Africa over the last half million years and implications for human evolution. *Proc. Natl. Acad. Sci. U. S. A.* **115**, 11174–11179 (2018).
8. S. J. Ivory, *et al.*, Environmental change explains cichlid adaptive radiation at Lake Malawi over the past 1.2 million years. *Proc. Natl. Acad. Sci. U. S. A.* **113**, 11895–11900 (2016).
9. T. Caley, *et al.*, A two-million-year-long hydroclimatic context for hominin evolution in southeastern Africa. *Nature* **560**, 76–79 (2018).
10. R. Tiedemann, M. Sarnthein, N. J. Shackleton, Astronomic timescale for the Pliocene Atlantic $\delta^{18}\text{O}$ and dust flux records of Ocean Drilling Program Site 659. *Paleoceanography* **9**, 619–638 (1994).
11. C. S. Miller, W. D. Gosling, D. B. Kemp, A. L. Coe, I. Gilmour, Drivers of ecosystem and climate change in tropical West Africa over the past ~540 000 years. *J. Quat. Sci.* **31**, 671–677 (2016).
12. J. Holtvoeth, T. Wagner, B. Horsfield, C. J. Schubert, U. Wand, Late-quaternary supply of terrigenous organic matter to the Congo deep-sea fan (ODP site 1075): Implications for equatorial African paleoclimate. *Geo-Marine Lett.* **21**, 23–33 (2001).
13. M. Zabel, T. Bickert, L. Dittert, R. R. Haese, Significance of the sedimentary Al:Ti ratio as an indicator for variations in the circulation patterns of the equatorial North Atlantic. *Paleoceanography* **14**, 789–799 (1999).
14. J. Etourneau, P. Martinez, T. Blanz, R. Schneider, Pliocene-Pleistocene variability of upwelling activity, productivity, and nutrient cycling in the Benguela region. *Geology* **37**, 871–874 (2009).
15. P. B. deMenocal, W. F. Ruddiman, E. M. Pokras, Influences of High- and Low-Latitude Processes on African Terrestrial Climate: Pleistocene Eolian Records from Equatorial Atlantic Ocean Drilling Program Site 663. *Paleoceanography* **8**, 209–242 (1993).
16. T. D. Herbert, *et al.*, Late Miocene global cooling and the rise of modern ecosystems. *Nat. Geosci.* **9**, 843–847 (2016).
17. M. Medina-Elizalde, D. W. Lea, The Mid-Pleistocene transition in the tropical Pacific. *Science* **310**, 1009–1012 (2005).
18. A. McIntyre, W. F. Ruddiman, K. Karlin, A. C. Mix, Surface water response of the equatorial Atlantic Ocean to orbital forcing. *Paleoceanography* **4**, 19–55 (1989).
19. G. Bräuer, The origin of modern anatomy: by speciation or intraspecific evolution? *Evol. Anthropol. Issues, News, Rev.* **17**, 22–37 (2008).
20. A. L. Deino, S. McBrearty, $^{40}\text{Ar}/^{39}\text{Ar}$ dating of the Kapthurin Formation, Baringo, Kenya. *J. Hum. Evol.* **42**, 185–210 (2002).
21. R. G. Klein, *The Human Career* (University of Chicago Press, 2009).
22. A. R. Millard, A critique of the chronometric evidence for hominid fossils: I. Africa and the Near East 500–50 ka. *J. Hum. Evol.* **54**, 848–874 (2008).
23. R. Potts, A. Deino, Mid-pleistocene change in large mammal faunas of east africa. *Quat. Res.* **43**, 106–113 (1995).

24. G. P. Rightmire, Patterns of hominid evolution and dispersal in the Middle Pleistocene. *Quat. Int.* **75**, 77–84 (2001).
25. G. P. Rightmire, Middle and later Pleistocene hominins in Africa and Southwest Asia. *Proc. Natl. Acad. Sci. U. S. A.* **106**, 16046–16050 (2009).
26. R. Grün, et al., Dating the skull from Broken Hill, Zambia, and its position in human evolution. *Nature*, 1–4 (2020).
27. O. M. Pearson, F. E. Grine, Re-analysis of the hominid radii from Cave of Hearths and Klasies River Mouth, South Africa. *J. Hum. Evol.* **32**, 577–592 (1997).
28. M. Lombard, C. Schlebusch, H. Soodyall, Bridging disciplines to better elucidate the evolution of early homo sapiens in southern africa. *S. Afr. J. Sci.* **109**, 1–8 (2013).
29. J. P. Raynal, F. Z. Sbihi Alaoui, L. Magoga, A. Mohib, M. Zouak, Casablanca and the earliest occupation of North Atlantic Morocco. *Quaternaire* **13**, 65–77 (2002).
30. F. L. Mendez, et al., An African American paternal lineage adds an extremely ancient root to the human y chromosome phylogenetic tree. *Am. J. Hum. Genet.* **92**, 454–459 (2013).
31. J. J. Hublin, et al., New fossils from Jebel Irhoud, Morocco and the pan-African origin of Homo sapiens. *Nature* **546**, 289–292 (2017).
32. D. Richter, et al., The age of the hominin fossils from Jebel Irhoud, Morocco, and the origins of the Middle Stone Age. *Nature* **546**, 293–296 (2017).
33. L. R. Berger, J. Hawks, P. H. G. M. Dirks, M. Elliott, E. M. Roberts, Homo naledi and Pleistocene hominin evolution in subequatorial Africa. *Elife* **6**, e24234 (2017).
34. P. H. G. M. Dirks, et al., The age of homo naledi and associated sediments in the rising star cave, South Africa. *Elife* **6**, e24231 (2017).
35. D. D. Stnyder, J. Moggi-Cecchi, L. R. Berger, J. E. Parkington, Human mandibular incisors from the late Middle Pleistocene locality of Hoedjiespunt 1, South Africa. *J. Hum. Evol.* **41**, 369–383 (2001).
36. C. Stringer, The origin and evolution of homo sapiens. *Philos. Trans. R. Soc. B Biol. Sci.* **371**, 20150237 (2016).
37. R. Grün, et al., Direct dating of Florisbad hominid. *Nature* **382**, 500–501 (1996).
38. L. R. Berger, J. Hawks, Revisiting the age of the Florisbad hominin material. *AfricArXiv* (2020).
39. J. Quade, J. G. Wynn, The Geology of Early Humans in the Horn of Africa (Geological Society of America, 2008).
40. I. McDougall, F. H. Brown, J. G. Fleagle, Sapropels and the age of hominins Omo I and II, Kibish, Ethiopia. *J. Hum. Evol.* **55**, 409–420 (2008).
41. G. Bräuer, R. Leakey, E. Mbua, A first report on the ER-3884 cranial remains from Ileret/East Turkana, Kenya. Contin. or Replace. *Controv. Homo sapiens Evol.*, 111–120 (1992).
42. E. Trinkaus, A note on the KNM-ER 999 hominid femur. *J. Hum. Evol.* **24**, 493–504 (1993).
43. G. Bräuer, Y. Yokoyama, C. Falgueres, E. Mbua, Modern human origins backdated. *Nature* **386**, 337–338 (1997).
44. J.-J. Hublin, “Northwestern African Middle Pleistocene hominids and their bearing on the emergence of Homo sapiens” in Human Roots: Africa and Asia in the Middle Pleistocene, L. Barham, K. Robson-Brown, Eds. (2001), pp. 99–121.
45. G. Bräuer, R. E. Leakey, The ES-11693 cranium from Eliye Springs, West Turkana, Kenya. *J. Hum. Evol.* **15**, 289–312 (1986).
46. G. Bräuer, et al., Virtual Study of the Endocranial Morphology of the Matrix-Filled Cranium from Eliye Springs, Kenya. *Anat. Rec. - Part A Discov. Mol. Cell. Evol. Biol.* **276**, 113–133 (2004).
47. J. D. Clark, et al., Stratigraphic, chronological and behavioural contexts of Pleistocene Homo sapiens from Middle Awash, Ethiopia. *Nature* **423**, 747–752 (2003).
48. T. D. White, et al., Pleistocene Homo sapiens from Middle Awash, Ethiopia. *Nature* **423**, 742–747 (2003).
49. K. Lubsen, R. Corruccini, Morphometric analysis of the Herto cranium (BOU-VP-16/1): Where does it fit? *J. Contemp. Anthropol.* **2**, 1 (2011).
50. R. McCarthy, L. Lucas, A morphometric re-assessment of BOU-VP-16/1 from Herto, Ethiopia. *J. Hum. Evol.* **74**, 11 (2014).
51. A. S. Woodward, A Fossil Skull of an Ancestral Bushman from the Anglo-Egyptian Sudan. *Antiquity* **12**, 190–195 (1938).

52. C. Stringer, L. Cornish, P. Stuart-Macadam, Preparation and further study of the Singa skull from Sudan. *Bull. Br. Museum, Nat. Hist. Geol.* **38**, 347–358 (1985).
53. F. Spoor, C. Stringer, F. Zonneveld, Rare temporal bone pathology of the Singa calvaria from Sudan. *Am. J. Phys. Anthropol.* **107**, 41–50 (1998).
54. F. McDermott, et al., New late-Pleistocene uranium-thorium and ESR dates for the Singa hominid (Sudan). *J. Hum. Evol.* **31**, 507–516 (1996).
55. M. Will, S. El-Zaatari, K. Harvati, N. J. Conard, Human teeth from securely stratified Middle Stone Age contexts at Sibudu, South Africa. *Archaeol. Anthropol. Sci.* **11**, 3491–3501 (2019).
56. F. E. Grine, “The late quaternary Hominins of Africa: The Skeletal evidence from MIS 6-2” in *Africa from MIS6-2: Population Dynamics and Paleoenvironments*, S. C. Jones, B. Stewart, Eds. (Springer, 2016), pp. 323–381.
57. G. Bräuer, M. J. Mehlman, Hominid molars from a middle stone age level at the Mumba Rock Shelter, Tanzania. *Am. J. Phys. Anthropol.* **75**, 69–76 (1988).
58. G. Bräuer, A. Mabulla, New hominid fossil from Lake Eyasi, Tanzania. *Anthropologie*, 47–53 (1996).
59. M. Domínguez-Rodrigo, et al., A new archaic *Homo sapiens* fossil from Lake Eyasi, Tanzania. *J. Hum. Evol.* **54**, 899–903 (2008).
60. J. J. Hublin, et al., “Dental Evidence from the Aterian Human Populations of Morocco” in *Modern Origins*, (Springer, 2012), pp. 189–204.
61. G. Avery, et al., The Ysterfontein 1 Middle Stone Age Rock Shelter and the Evolution of Coastal Foraging. *Goodwin Ser.*, 66–89 (2008).
62. M. H. Day, M. D. Leakey, C. Magori, A new hominid fossil skull (L.H. 18) from the Ngaloba Beds, Laetoli, northern Tanzania. *Nature* **284**, 55–56 (1980).
63. M. Grove, et al., Climatic variability, plasticity, and dispersal: A case study from Lake Tana, Ethiopia. *J. Hum. Evol.* **87**, 32–47 (2015).
64. P. Cohen, Fitting a face to Ngaloba. *J. Hum. Evol.* **30**, 373–379 (1996).
65. G. P. Rightmire, Comparison of Middle Pleistocene hominids from Africa and Asia. *Hum. Roots Africa Asia Middle Pleistocene*, 123–133 (2001).
66. K. Harvati, J. J. Hublin, “Morphological Continuity of the Face in the Late Middle and Late Pleistocene Hominins from Northwestern Africa: A 3D Geometric Morphometric Analysis” in *Modern Origins*, (Springer, 2012), pp. 179–188.
67. R. N. E. Barton, A. Bouzouggar, S. N. Collcutt, J. L. Schwenninger, L. Clark-Balzan, OSL dating of the Aterian levels at Dar es-Soltan I (Rabat, Morocco) and implications for the dispersal of modern *Homo sapiens*. *Quat. Sci. Rev.* **28**, 1914–1931 (2009).
68. M. L. McCrossin, Human molars from later Pleistocene deposits of Witkrans Cave, Gaap Escarpment, Kalahari Margin. *Glob. Bioeth.* **7**, 1–10 (1994).
69. F. E. Grine, R. G. Klein, Late Pleistocene human remains from the Sea Harvest site, Saldanha Bay, South Africa. *S. Afr. J. Sci.* **89**, 145–146 (1993).
70. Y. Haile-Selassie, B. Asfaw, T. D. White, Hominid Cranial Remains from Upper Pleistocene Deposits at Aduma, Middle Awash, Ethiopia. *Am. J. Phys. Anthropol.* **123**, 1–10 (2004).
71. F. E. Grine, R. G. Klein, Pleistocene and Holocene human remains from Equus cave, South Africa. *Anthropology* **8**, 55–98 (1985).
72. F. E. Grine, Middle Stone Age human fossils from Die Kelders Cave 1, Western Cape Province, South Africa. *J. Hum. Evol.* **38**, 129–145 (2000).
73. P. M. Vermeersch, et al., A middle palaeolithic burial of a modern human at Taramsa hill, Egypt. *Antiquity* **72**, 475–484 (1998).
74. P. Van Peer, P. Vermeersch, E. Paulissen, Chert Quarrying, Lithic Technology, and a Modern Human Burial at the Palaeolithic Site of Taramsa 1, Upper Egypt (Leuven University Press, 2010).
75. R. Grün, P. Beaumont, P. V. Tobias, S. Eggins, On the age of Border Cave 5 human mandible. *J. Hum. Evol.* **45**, 155–167 (2003).
76. K. Douka, et al., The chronostratigraphy of the Haua Fteah cave (Cyrenaica, northeast Libya). *J. Hum. Evol.* **66**, 39–63 (2014).
77. F. E. Grine, C. S. Henshilwood, Additional human remains from Blombos Cave, South Africa: (1999–2000 excavations). *J. Hum. Evol.* **42**, 293–302 (2002).

78. W. B. Reiner, et al., OH 83: A new early modern human fossil cranium from the Ndutu beds of Olduvai Gorge, Tanzania. *Am. J. Phys. Anthropol.* **164**, 533–545 (2017).
79. F. E. Grine, et al., Late pleistocene human skull from Hofmeyr, South Africa, and modern human origins. *Science* **315**, 226–229 (2007).